Nature of the Spin Dynamics and 1/3 Magnetization Plateau in Azurite

K. C. Rule,[1] A. U. B. Wolter,[1] S. Süllow,[2] D. A. Tennant,[1] A. Brühl,[3] S. Köhler,[3] B. Wolf,[3] M. Lang,[3] and J. Schreuer[4]

[1]*Hahn-Meitner-Institut GmbH, D-14109 Berlin, Germany*

[2]*Inst. für Physik der Kondensierten Materie, TU Braunschweig, D-38106 Braunschweig, Germany*

[3]*Physikalisches Institut, J.W. Goethe-Universität Frankfurt, D-60438 Frankfurt(M), Germany*

[4]*Ruhr-Universität Bochum, Bochum, Germany*

(Received 11 September 2007; published 19 March 2008)

We present a specific heat and inelastic neutron scattering study in magnetic fields up into the 1/3 magnetization plateau phase of the diamond chain compound azurite $Cu_3(CO_3)_2(OH)_2$. We establish that the magnetization plateau is a dimer-monomer state, i.e., consisting of a chain of $S = 1/2$ monomers, which are separated by $S = 0$ dimers on the diamond chain backbone. The effective spin couplings $J_{\mathrm{mono}}/k_B = 10.1(2)$ K and $J_{\mathrm{dimer}}/k_B = 1.8(1)$ K are derived from the monomer and dimer dispersions. They are associated to microscopic couplings $J_1/k_B = 1(2)$ K, $J_2/k_B = 55(5)$ K and a ferromagnetic $J_3/k_B = -20(5)$ K, possibly as result of d_{z^2} orbitals in the Cu-O bonds providing superexchange (SE) pathways with $J_{\mathrm{SE}} = 6.5$ K.

DOI: 10.1103/PhysRevLett.100.117202 PACS numbers: 75.30.Et, 75.10.Pq, 75.45.+j

Great interest has surrounded the observation of a 1/3 magnetization plateau in azurite $Cu_3(CO_3)_2(OH)_2$ [1,2]. This material, famous as a painting pigment of deep-blue color, has been proposed as a realization of the exotic diamond chain of coupled spin-1/2 moments [3–5] (see sketch Fig. 3). Here, J_2 is the magnetic coupling of the diamond backbone, while J_1 and J_3 represent the coupling of the monomers along the chain. Depending on the relative coupling strengths J_1, J_2, J_3 this model affords a host of exotic phases and quantum phase transitions, including $M = 1/3$ fractionalization [6] or exotic dimer phases [4]. We believe that the delicate balance between the interactions J_1, J_2 and J_3 in azurite reveals an in depth understanding of the physics of 1/3 magnetization plateaus in trimer spin systems.

Controversy surrounds the issue of magnetic exchange in azurite. While a susceptibility χ study claims antiferromagnetic coupling for J_1, J_2, J_3 implying strong frustration [1], subsequent numerical studies of χ dispute this claim, proposing a ferromagnetic (FM) J_3, and thus a nonfrustrated scenario [2]. These starkly contrasting interpretations of the same data directly relate to the nature of magnetic coupling. In azurite $Cu_3(CO_3)_2 \times (OH)_2$, the Cu^{2+} ions ($S = 1/2$) are in a square-planar coordination on two inequivalent sites [7]. With a monoclinic crystal structure (space group $P2_1/c$, lattice parameters $a = 5.01$ Å, $b = 5.85$ Å, $c = 10.3$ Å, $\beta = 92.4°$ [8,9]), the Cu^{2+} network forms diamond-shaped units arranged in chains running along the b direction. The magnetic exchange pathways for the J_1, J_2 and J_3 couplings are along Cu-O-Cu bonds with angles of 113.7°, 97°, and 113.4°, respectively. Hence, the Goodenough-Kanamori-Anderson rules for superexchange [10] would predict weakly antiferromagnetic (AFM) couplings [11].

However, this conclusion is only valid if the magnetic orbitals are dominantly $d_{x^2-y^2}$ character. If the Cu orbitals tend to be more d_{z^2} like, higher-order effects can give rise to FM exchange [12]. The latter case may become relevant for systems with bond angles away from the limiting cases of 90° and 180°, such as CuO [13]. Recent x-ray diffraction experiments [9] on azurite hint at an electronic configuration in which d_{z^2} like contributions play a major role, making azurite another prominent candidate for such superexchange interactions.

In this Letter we present a detailed study of azurite by means of specific heat and inelastic neutron scattering (INS) in zero and applied magnetic field. We investigate the elementary magnetic excitations and estimate the microscopic coupling constants. In particular, we establish the nature of the plateau phase by determining the $\mathbf{q}$ dependence of its spin-excitation spectrum. Specific heat $C_p(T)$ measurements at temperatures 1.6 to 30 K were carried out using an ac-calorimeter [14] on an azurite crystal (mass: 0.36 mg), which was cut from the crystal used for neutron scattering. An external field up to 4 T was oriented in the ac-plane, and 65° away from the c axis. This orientation corresponds approximately to the easy axis of the AFM phase below $T_N = 1.85$ K [15]. The $C_p(T)$ results are displayed in Fig. 1 up to 10 K. Beside the AFM transition, indicated by a sharp discontinuity, the zero-field data reveal a broad maximum around 3.7 K. At $B = 4$ T the maximum becomes reduced in size and shifted to lower temperatures.

The starting point of our analysis is the *dimer-monomer* model proposed in Ref. [4], with the intradimer coupling constant J_2 representing the dominant energy scale. At temperatures $T < 10$ K, considered here for the specific heat, and for $J_2/k_B \gg 10$ K (see below), the magnetic degrees of freedom of azurite are dominated by the chain of spin-1/2 Cu^{2+}-monomers, which are antiferromagnetically coupled via the rungs of the diamond backbone [1]. Using the magnetic specific heat C_{AFHC} of the AFM $S = 1/2$ Heisenberg chain (AFHC) [16], and including a lattice contribution $C_{\mathrm{lat}} \propto (T/\Theta_D)^3$, the zero-field specific heat

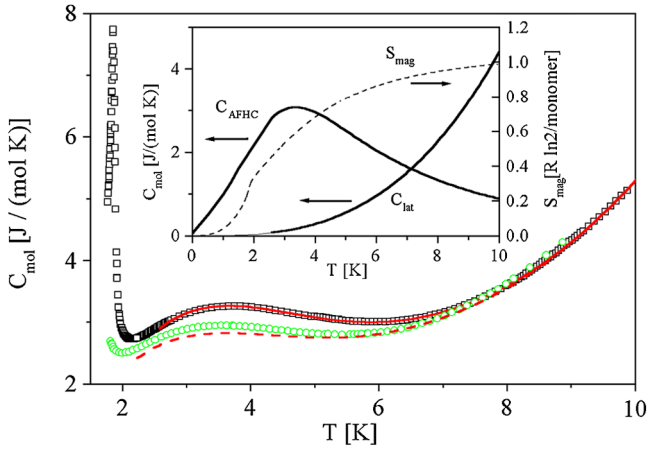

FIG. 1 (color online). $C_p(T)$ of a single crystal of azurite for $B = 0$ T (□) and 4 T (○). The solid (dashed) line represents a fit to the zero-field ($B = 4$ T) data [16] (see text). The inset shows $C_{\mathrm{AFHC}}(T, B = 0)$, C_{lat} and S_{mag} derived by integrating $C_p(T) - C_{\mathrm{lat}}(T)/T$ where C_p for $T < T_N$ was extrapolated using a T^3 term for the AFM magnons.

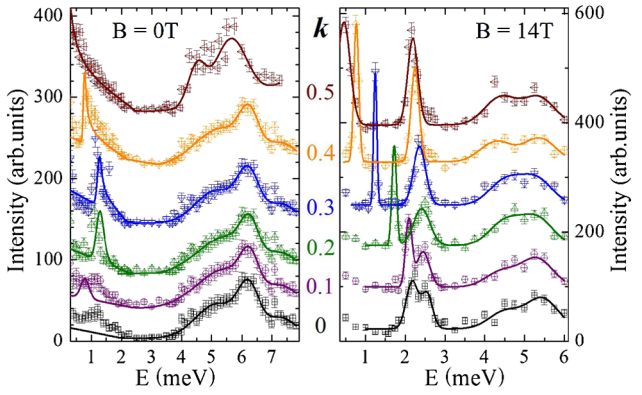

FIG. 2 (color online). Energy dependence of the INS spectra of azurite at $\mathbf{q} = (1, k, 0)$, $k = 0$ to 0.5, in zero field (left) and a field of 14 T $\perp b^*$ (right) at $T = 1.5$ K. Lines indicate fits to the data, which are shifted for clarity; for details see text.

$C_p(T)$ is well fitted down to 2.5 K. In this fit, the magnetic coupling $J_{\mathrm{AFHC}}/k_B = 7.0(1)$ K and a Debye temperature $\Theta_D = 188$ K were used (solid line in Fig. 1). The corresponding magnetic entropy S_{mag}, normalized to a Cu^{2+} monomer, reaches the full value $R \ln 2$ at about 10 K (broken line in the inset of Fig. 1). Using the same lattice contribution and $C_{\mathrm{AFHC}}(T, B)$ results calculated for the AFHC in finite field [16], this ansatz (broken line in Fig. 1) also captures the main features of the experimental data at $B = 4$ T.

INS was used to further probe the character of the magnetic excitations both at zero and high magnetic field. To avoid thermal line broadening and adverse effects from the structural distortion observed at 1.86 K, care was taken to maintain the sample temperature at $T = 1.5$ K. Experiments were carried out at the Berlin Neutron Scattering Center using the V2 cold-neutron triple-axis spectrometer. Constant-**Q**, energy transfer scans in a range 0–7.8 meV were performed with incident neutrons fixed at $k_i = 1.55$ and 1.3 $\mathrm{Å}^{-1}$ which gave an energy resolution of 0.15 and 0.11 meV, respectively. A large (>15 g), naturally grown azurite single crystal was mounted with a horizontal a^*-b^* scattering plane, and magnetic fields of up to 14 T applied perpendicular to b^*. Susceptibility data, taken on pieces of this crystal, perfectly reproduce the results reported in Ref. [1].

Figure 1 shows the energy dependence of the scattering intensity for various positions $\mathbf{q} = (1, k, 0)$ along the diamond chain in 0 and 14 T, i.e., in the 1/3 magnetization plateau phase between $B_{c1} = 11$ T and $B_{c2} = 30$ T. Because of symmetric behavior about $k = 0.5$, only data in the range $0 \le k \le 0.5$ are shown.

Along $\mathbf{q} = (1, k, 0)$ and in zero magnetic field, there is scattering intensity at energies <2 meV displaying the $|\sin \mathbf{q}|$ dependence of an $S = 1/2$ AFHC (left panel Fig. 2). The fits shown were produced by combining Gaussian line shapes for the features above 2 meV, while those below 2 meV were calculated using a 1D chain [17] convolved with instrumental resolution and the copper form factor. The fit yields an effective magnetic coupling strength of $J_{\mathrm{AFHC}}/k_B = 9(1)$ K (solid lines <2 meV). The difference between J_{AFHC} measured from specific heat and INS is not well understood and will require additional studies. Perpendicular to the chain, i.e., along $[h\ 0.5\ 0]$, within experimental resolution there is no dispersion (not shown), consistent with the 1D nature of these spin excitations. Further, our spectra reveal a broad peak structure at energies above 3.5 meV in zero magnetic field (left panel Fig. 2). As we will argue, this feature arises from singlet-triplet excitations of the spin dimers on the backbone of the diamond chain structure.

Within the *dimer-monomer* model, the monomer chain becomes fully polarized at the lower critical field B_{c1} of the plateau phase. Correspondingly, a gap opens at the AFM point $\mathbf{q} = (1\ 0.5\ 0)$. The excitations are now ferromagnons, yielding scattering intensity with a cosinusodial dispersion (see low-energy peak $0.4 \le E \le 2.2$ meV in 14 T; right panel Fig. 2). By fitting the peak positions using Gaussian profiles as indicated in the plot, we extract the $E(k)$ dependence in Fig. 3 (black squares). The data are parameterized by an expression $E(k) = g_{\mathrm{av}} \mu_B B + J_{\mathrm{mono}}[\cos(2\pi k) - 1] + \Delta_{\mathrm{chain}}$. With $g_{\mathrm{av}} = 2.1$ from ESR measurements [18] and $\Delta_{\mathrm{chain}} = 0.53$ meV, we obtain the effective magnetic coupling $J_{\mathrm{mono}}/k_B = 10.1(2)$ K. Higher order cosine terms do not improve the fitting, resulting in 0.2 K as upper boundary for next-nearest-monomer interactions.

The broad peak in the spectra above 3.5 meV in Fig. 2 is attributed to singlet-triplet excitations within the dimers. In magnetic fields, Zeeman splitting lifts the zero-field degeneracy of the singlet-triplet peak, lowering the $|\uparrow\uparrow\rangle$ triplet branch in energy and separating it from the broad structure. Accordingly, in $B = 14$ T, a weakly dispersive peak is observed at ~2.2–2.5 meV (right panel Fig. 2). By fitting

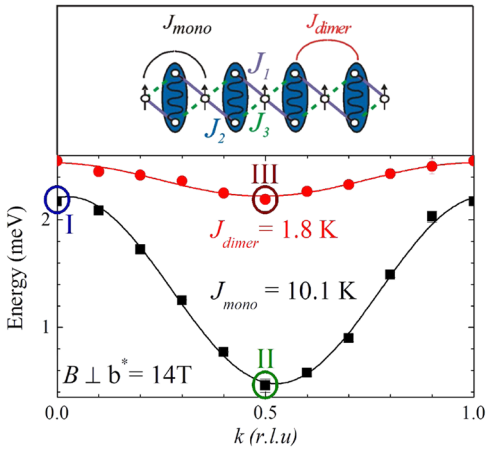

FIG. 3 (color online). (Top) *Dimer-monomer* model with microscopic couplings J_1, J_2, J_3, and effective couplings J_{mono}, J_{dimer}, characterizing the plateau phase. (Bottom) $E(k)$ dependence along $\mathbf{q} = (1, k, 0)$ for the two low-lying excitations in $B(\perp b^*) = 14$ T. Lines are fits to the data, see text. The small asymmetry of the data around $k = 0.5$ reflects a slight misalignment of the crystal. Highlights I, II, III indicate positions investigated for their B dependence in Fig. 4.

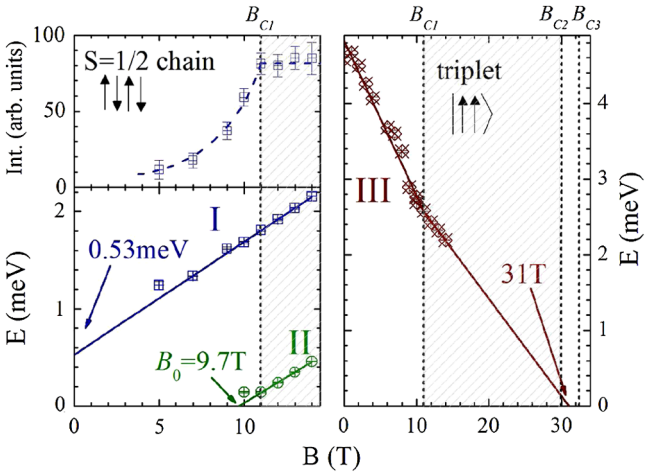

FIG. 4 (color online). (Left) B dependence of the integrated peak intensity (top) and monomer energy (bottom) at $\mathbf{q} = (1\ 0\ 0)$ (I) and $(1\ 0.5\ 0)$ (II). (Right) energy of the low-lying triplet branch ($|\uparrow\uparrow\rangle$) at $\mathbf{q} = (1\ 0.5\ 0)$ (III) as function of B. Hatched region indicates the plateau phase. Solid lines: fits to the data; dashed lines, guides to the eye.

the peak positions of the low-lying triplet using Gaussian profiles, we extract the $E(k)$ dependence in Fig. 3 (red circles). It can be parameterized by $E(k) = -g_{\mathrm{av}}\mu_B B + J_2 + J_{\mathrm{dimer}}\cos(2\pi k) + \mu_B \tilde{b}$, with $g_{\mathrm{av}} = 2.1$ [18] and J_2 as zero-field singlet-triplet splitting. The parameter $\tilde{b}$ accounts for the internal field shift at the dimer site due to the alignment of neighboring monomers. From the width of the dispersion we obtain an effective dimer-dimer coupling $J_{\mathrm{dimer}} = 1.8$ K. The other triplet branches, even in highest fields, superimpose and yield a broad distribution of scattering intensity above 3.5 meV, prohibiting a precise determination of peak positions. As yet, the cause for the peak broadening of these branches is not understood.

The critical fields of the plateau phase are extracted from a field-dependent study of the monomer and lowest dimer excitations. First, we note that the field dependence of the monomer dispersion should be that of the $S = 1/2$ AFHC. Hence, at $\mathbf{q} = (1\ 0\ 0)$ (marker I in Fig. 3) a (close to) linear-in-field behavior is expected, which is gapless in zero field [19]. As shown in the lower left panel of Fig. 4, a linear behavior is in fact observed experimentally. Further, $B_{c1} = 11$ T is identified in the field dependence of the peak intensity (upper left panel Fig. 4) as a distinct kink. The intensity is constant above B_{c1}, but it falls off rapidly with decreasing field for $B < B_{c1}$. The intensity decrease is due to the first moment sum rule and is related to the magnetization [20].

Surprisingly, an extrapolation of the peak position for $B \geq B_{c1}$ to zero field yields a finite gap $\Delta_{\mathrm{chain}} = 0.53$ meV. This feature also accounts for the mismatch at low energies between fit and data at $\mathbf{q} = (1\ 0\ 0)$ in zero field (left panel Fig. 2). Unfortunately, a detailed study of this behavior is hampered by the strong reduction of peak intensity (upper left panel Fig. 4). The AFM ordered state may affect the behavior of the monomer chain, leading to a zero-field gap at the nuclear zone center. Certainly, this issue calls for further investigations.

The B dependence of the monomer peak at $(1\ 0.4\ 0)$ was also measured. Assuming a $\cos(2\pi k)$ dependence of $E(k)$, we approximate the field dependence of the $E(k)$ minimum at $(1\ 0.5\ 0)$ (marker II in Fig. 3), this way accessing the field of gap closure for the ferromagnons [21]. For $B \geq B_{c1}$ the expected linear-in-field behavior of the gap is observed experimentally, with an extrapolated field of gap closure $B_0 = 9.7$ T (lower left panel Fig. 4). We associate the difference between B_{c1} and B_0 to the local mean field due to the AFM order.

Our data suggest that the magnetization plateau reaches from the field B_{c1} of full monomer polarization up to B_{c2}, where the low-lying triplet $|\uparrow\uparrow\rangle$ reaches zero energy. Moreover, Zeeman splitting results in a dependence $\propto B$ for this triplet branch. To test this, we have measured the field dependence of the $|\uparrow\uparrow\rangle$ branch at the minimum $\mathbf{q} = (1\ 0.5\ 0)$ (marker III in Fig. 3; data in Fig. 4, right panel). As expected, for fields $B \geq B_{c1}$ a linear field dependence is observed. An extrapolation to zero energy from the low-lying triplet $|\uparrow\uparrow\rangle$ at $\mathbf{q} = (1\,0.5\,0)$ yields 31 T, which closely matches the value $B_{c2} = 30$ T reported as upper critical field of the magnetization plateau. Extrapolating to zero energy for $\mathbf{q} = (1\ 0\ 0)$ gives $B_{c3} = 33.6$ T also comparable to the reported value [1] of 32.5 T for the onset of magnetization saturation to the full moment. Below B_{c1}, for the triplet $|\uparrow\uparrow\rangle$ at $\mathbf{q} = (1\ 0.5\ 0)$ a behavior $\propto B$, but with a steeper negative slope, is observed. This reflects the presence of local molecular fields in the AFM ordered state. Fitting the data at $B \leq B_{c1}$ yields a zero-field singlet-triplet

splitting of 4.8(5) meV [$\sim$55(5) K], which essentially corresponds to the magnetic coupling J_2.

Altogether, our data reveal that the magnetization plateau in azurite arises out of the *dimer-monomer* state proposed in Ref. [4] with the chain of AFM coupled $S = 1/2$ monomers fully polarized in the plateau phase. Low order perturbation theory implies that $J_{\mathrm{mono}}/J_{\mathrm{dimer}} = 2$, however, experimentally this is $\sim$6. The addition of a superexchange (SE) interaction $J_{\mathrm{SE}} = 6.5$ K through the Cu-O-O-Cu pathway can account for this discrepancy such that $J_{\mathrm{mono}} = J_{\mathrm{SE}} + 2J_{\mathrm{dimer}}$. This type of process is not unusual in cuprate systems.

The first-order perturbation theory, relates analytical expressions for J_2, J_{dimer} to the microscopic couplings J_1, J_3 provided that $J_2 \gg J_1$, J_3 [5]. Although in azurite the latter condition might not be strictly fulfilled, our data indicate J_2 to be the strongest coupling. Employing J_2 and J_{dimer} from experiment and following Ref. [5], we approximate J_1 and J_3 from two conditions. (I) For the dimer coupling it predicts $J_{\mathrm{dimer}} \approx (J_1 - J_3)^2/4J_2$. (II) The change in slope of the dimer dispersion at B_{c1} (Fig. 4) arises from a change in local mean fields from AFM to FM. Extrapolating the data at $B > B_{c1}$ to zero field we obtain the difference between FM and AFM polarization $\Delta E \approx (J_1 + J_3)/2 + J_{\mathrm{dimer}} = -0.8$ meV. The consistency of our calculations we check by using the various critical field expressions such as $B_{c2} \approx [J_2 - J_{\mathrm{dimer}} + (J_1 + J_3)/2]/g_{av}\mu_B$. Condition I. restricts parameter space for J_1 and J_3, condition II. requires J_1 and J_3 to have opposite sign. As an optimum solution we obtain $J_3/k_B \simeq -20(5)$ K and $J_1/k_B \simeq 1(2)$ K.

Our most important conclusion is that of a FM coupling in azurite, as was suggested previously [2]. The J_3 path has Cu-O-Cu exchange along one filled and one unfilled orthogonal orbital, with atomic Cu-O distances of 1.947 and 1.989 Å separated by an angle of 113.4°. By reducing the Anderson superexchange mechanism and with the Cu orbitals possibly dominated by a d_{z^2} character [9], direct exchange and oxygen Hund's rule coupling can yield a substantial ferromagnetic exchange pathway [12].

The values of J_2, J_3 are in agreement with Ref. [2], and these two couplings appear to control the susceptibility with its two-maxima structure. As well, the properties of the high field plateau phase in essence are accounted for within a model invoking two J values [(J_{mono}, J_{dimer}), or (J_2, J_3, J_{SE})]. Moreover, compared to the Refs. [1,2], our much more detailed $\mathbf{q}$, energy and field-dependent neutron scattering data imply $|J_1| \ll |J_2|$, $|J_3|$ and thus frustration effects will be absent or weak. J_1 represents a weak perturbation, and is possibly less important than other factors such as the Dzyaloshinskii-Moriya-interaction [1]. Here, additional experiments in lower fields and at lower energies will be necessary to assess the relevance of these different factors.

To conclude, we have studied the distorted diamond chain model system azurite $Cu_3(CO_3)_2(OH)_2$ by means of specific heat and inelastic neutron scattering. The magnetization plateau can be understood within the *dimer-monomer* model from Ref. [4]. For the microscopic couplings J_1, J_2, and J_3 within the diamond units we find J_2 and J_3 to be dominant, with J_3 being ferromagnetic. Accounting for this type of superexchange ought to be possible along the lines set out in Ref. [12]. Given the limits of our perturbative analytic approach, further calculations, which take the renormalization of magnetic couplings by quantum fluctuations into account, are needed to fully model the distorted diamond chain azurite $Cu_3(CO_3)_2(OH)_2$.

This work was supported by BENSC and SFB/TRR 49. We thank H. Mikeska, A. Honecker, J. Richter, S. Großjohann, and W. Brenig for fruitful discussions.

[1] H. Kikuchi *et al.*, Phys. Rev. Lett. **94**, 227201 (2005).
[2] B. Gu and G. Su, Phys. Rev. Lett. **97**, 089701 (2006).
[3] K. Takano, K. Kubo, and H. Sakamoto, J. Phys. Condens. Matter **8**, 6405 (1996).
[4] K. Okamoto, T. Tonegawa, and M. Kaburagi, J. Phys. Condens. Matter **15**, 5979 (2003).
[5] A. Honecker and A. Läuchli, Phys. Rev. B **63**, 174407 (2001).
[6] M. Oshikawa, M. Yamanaka, and I. Affleck, Phys. Rev. Lett. **78**, 1984 (1997).
[7] B. J. Reddy and K. B. N. Sarma, Solid State Commun. **38**, 547 (1981).
[8] G. Gattow and J. Zemann, Acta Crystallogr. **11**, 866 (1958); F. Zigan and H. D. Schuster, Z. Kristallogr. **135**, 416 (1972).
[9] E. L. Belokoneva, Y. K. Gubina, and J. B. Forsyth, Phys. Chem. Miner. **28**, 498 (2001).
[10] P. W. Anderson, Phys. Rev. **115**, 2 (1959).
[11] The J_2 bond angle is close to FM exchange, but proven to be AFM by experiment; see Ref. [1].
[12] A. Filippetti and V. Fiorentini, Phys. Rev. Lett. **95**, 086405 (2005).
[13] B. X. Yang, T. R. Thurston, J. M. Tranquada, and G. Shirane, Phys. Rev. B **39**, 4343 (1989); T. Shimizu *et al.*, *ibid.* **68**, 224433 (2003).
[14] P. F. Sullivan and G. Seidel, Phys. Rev. **173**, 679 (1968).
[15] R. D. Spence and R. D. Ewing, Phys. Rev. **112**, 1544 (1958); N. D. Love *et al.*, Phys. Lett. A **33**, 290 (1970).
[16] A. Klümper, Eur. Phys. J. B **5**, 677 (1998).
[17] J.-S. Caux and R. Hagemans, J. Stat. Mech. (2006) P12013.
[18] M. Ishii *et al.*, J. Phys. Soc. Jpn. **69**, 340 (2000); H. Ohta *et al.*, J. Phys. Soc. Jpn. **72**, 2464 (2003).
[19] A. Klümper and D. C. Johnston, Phys. Rev. Lett. **84**, 4701 (2000).
[20] P. C. Hohenberg and W. F. Brinkman, Phys. Rev. B **10**, 128 (1974).
[21] This position was not accessible directly because of the incoherent elastic scattering.